IEEE Journal of Photovoltaics, Volume 10, Issue 5, September 2020, pp. 1503-1507
DOI:10.1109/JPHOTOV.2020.2999881

Simulation of CZTSSe thin film solar cells in COMSOL: 3D coupled optical, electrical, and thermal model

Soma Zandi[a], Prateek Saxena[b], Mohammad Razaghi[a], Nima E. Gorji[c,*]

[a] *Department of Electrical Engineering, Faculty of Engineering, University of Kurdistan, Sanandaj, Iran*
[b] *Sustainable Manufacturing Systems Centre, School of Aerospace, Transport and Manufacturing, Cranfield University, Bedfordshire, UK*
[c] *Faculty of Electrical and Electronics Engineering, Ton Duc Thang University, Ho Chi Minh City, VietNam*

Abstract

The $Cu_2ZnSnS_xSe_{4-x}$ (CZTSSe) thin film solar cells have attracted the attention of researchers due to it's earth-abundant composition containing Copper, Zinc, Tin and Sulfur and Selenide with 12.6% record efficiency (2013-IBM). A 3D simulation analysis is presented here on the optical, electrical and thermal characteristics of CZTSSe solar cell using COMSOL Multiphysics 3D simulation package. COMSOL is capable of calculating the coupled optical-electrical-thermal models through Electromagnetic Wave, Semiconductor, and Heat Transfer modules for a finely meshed structure. Using this capability, we have calculated the optical photo-generation rate of the a Mo/Mo(S,Se)$_2$/CZTSSe/CdS/ZnO/ITO/air structure by inserting the refractive index and extinction coefficient of every layer in Wave optic module in COMSOL. We also calculated the total optical generation rate for two structures with and without Mo(S,Se)$_2$ layer at the junction of Mo and CZTSSe layers. The current-voltage curve, electric field profile and the recombination rate of the cell has also been calculated by Semiconductor module coupled to wave optic module. The current-voltage characteristics shows an improvement in V_{oc} for the cell with Mo(S,Se)$_2$ layer (0.46 V to 0.513 V) which was also suggested by IBM for a record cell efficiency. Finally, the thermal maps of the cell has been calculated by Heat Transfer Module coupled to Semiconductor module considering the Shockley-Read-Hall (SRH) recombination heat, Joule Heat and conductive heat flux. The total heat flux magnitude of the cell was also mapped as a result out of these heat generation and cooling sources. The SRH heat is maximum within the depletion width at the CZTSSe/CdS interface whereas the Joule heating is intensive at the Mo/Mo(S,Se)$_2$/CZTSSe side. Interesting is to see that the heat is mainly conducted to environment from Mo side presented by the conductive heat map. The total heat flux is intensive at both top and bottom interfaces which means the heat is generated at both top and bottom sides of the cells and not only from the illuminated part.

Keywords: CZTSSe, Thin films, Solar cell, COMSOL,3D Simulation.

1. Introduction

Kesterite Thin film solar cells (based on CZTSSe materials) attracted the attention of many research groups as an alternative material for Cu(In,Ga)Se$_2$ chalcogenides since In is not an abundant element in earth. CZTSSe thin films have slowly raised their efficiency from 8% to 12% within few years [1]. The record efficiency of 12.6% patented by IBM company in 2013 has not been beaten yet [2]. The current challenge with CZTSSe devices is the low open-circuit voltage (V_{oc}) of 0.513 V (IBM-2013). This shows a large difference of $(E_g/q) - V_{oc}$ in compare to CIGSSe solar cells reported in [2, 3]. Currently, the low open-circuit voltage of CZTSSe solar cells is low (513 mV) compared to CdTe and CIGS thin film cells which is around 900-1000 mV. Fabrication process, phase formation, grain size and morphology of these cells are still under excessive research by many research groups [4, 5]. However, modeling and simulation analysis are also reported in the literature to gain insight into the photo-absorption, carrier generation, carrier transport and thermal stability of such devices [3, 6, 7]. Most of these simulation analysis have been performed by 1D simulation platforms such as SCAPS or AMPS which cannot consider the 3D features of a solar cell [8, 9]. However, 1D simulators do not allow thermal analysis and mapping the heat distribution or heat emission to environment and conduction to other layers. COMSOL multiphysics simulation package has been rarely used for simulation of CZTSSe devices [10, 11]. COMSOL contains semiconductor module for solving the drift-diffusion model of the carrier transport and also the Electromagnetic Waves module to map the optical photo-generation of the cell, as well as the heat-transfer module for thermal distribution mapping across the device structure [12]. COMSOL also allows to couple these modules to simultaneously map the photo-generation, recombination and the heat profile of the cell under the operation condition and in 3D mode. We have recently developed a coupled optical-electrical-thermal module for the perovskite solar

* *Email address:* Corresponding author: nimaegorji@tdtu.edu.vn (Nima E. Gorji)

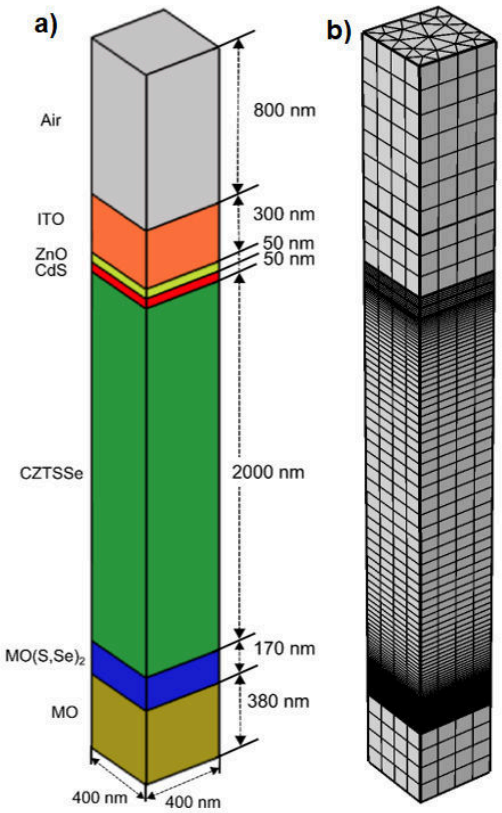

Figure 1: a. The schematic and geometry of the CZTSSe thin film solar cell as described in Ref. [2], and, b. the meshed structure.

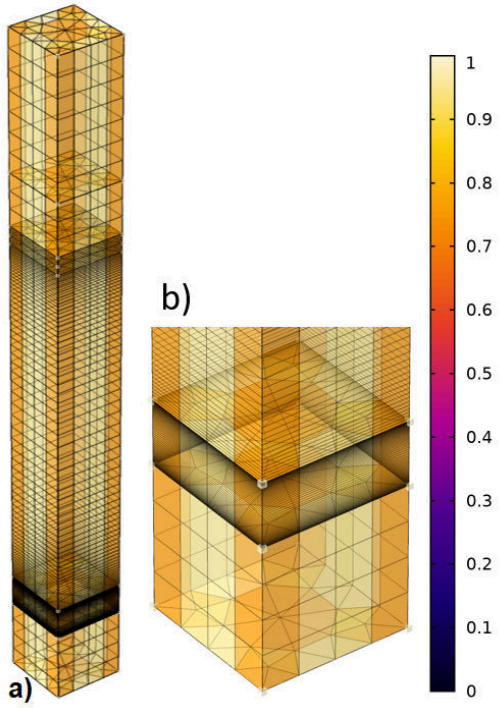

Figure 2: a. The mesh quality for skewness (overall geometry), and b. Mesh quality for $Mo(S,Se)_2$ layer

cell including a cell with reduced Graphene oxide electrode [13, 14].

In this paper, we present our numerical simulation analysis of the carrier transport, optical generation and thermal/heat distribution map of the CZTSSe thin film solar cells using COMSOL package. The optical generation rate across the cell structure, electric field profile, recombination rate and it's impact on device performance, as well as the heat distribution at a static steady-state has been simulated. We present a 3D analysis by solving a coupled optical-electrical-thermal profiles which has been rarely presented in literature. The two structures were compared in this paper: the cell with and without $Mo(S,Se)_2$ layer at the bottom junction of Mo and CZTSSe layers. This layer was suggested by IBM in 2013 to improve the open-circuit voltage of the cell without losing the short-circuit current density.To our best of knowledge, it's the first time that the thermal mapping of a CZTSSe thin film solar cell (at least in 3D) has been presented in literature.

2. Physics, Mesh & Simulation

The $Cu_2ZnSnS_xSe_{4-x}$ (CZTSSe) thin film solar cell is modelled using COMSOL Multiphysics 5.4a. Fig. 1 shows the device structure which is made of up to seven layers on a glass substrate (not shown here). We selected the structure presented in a reputed literature report in Ref. [2] given by $Mo/Mo(S,Se)_2/CZTSSe/CdS/ZnO/ITO$ structure which has given the world record efficiency of 12.6%. We have calculated the coupled optical and electrical simulation to include in the photo-absorption, carrier photo-generation, carrier collection, and efficiency of this device. For this purpose three multi-physics modules were coupled namely, Electromagnetic Waves (Frequency domain), Semiconductor module, and the Heat Transfer in Solid modules. The Electromagnetic Waves module required the optical constants, illumination intensity and the perfect conductors properties to calculated the total photo-generation (G_{tot}). The semiconductor module required the materials and electrical parameters and includes the trap assisted recombination and Shockley-Read-Hall: SRH recombination. This module uses the G_{tot} to solve the current-continuity equation as a result of coupling with Semiconductor and Electromagnetic wave modules. Heat transfer in solid module required the heat coefficients of the layers as listed in Table 1 and calculates the Joule heat, SRH heat and temperature distribution across the cell structure. The thermal/heat coefficients were taken from appropriate references. The heat coefficient of Mo was taken from Ref. [15, 16].

2.1. Model Geometry

The solar cell model is made up of seven layers in total. The top-most layer is modelled as air, extending up to 800 nm in height. The input power of the plane wave

Table 1: The values of selected electrical and thermal parameters used in COMSOL as partially reported in Refs. [2, 15, 16, 17, 18, 19, 23]

Parameter	Mo	$Mo(S,Se)_2$	CZTSSe	CdS	ZnO	ITO
Thickness (nm)	380	170	2000	50	50	300
ε_r	-	10	13.6	9	9	9
$N_c(cm^{-3})$	-	0.7×10^{18}	2.2×10^{18}	2.2×10^{18}	2.2×10^{18}	-
$N_v(cm^{-3})$	-	0.3×10^{19}	1.8×10^{19}	1.8×10^{19}	1.8×10^{19}	-
$\mu_n/\mu_p(cm^2/(V.s))$	-	100/25	100/25	100/25	100/25	-
χ(eV)	-	4.14	4.2	4.2	4.4	-
Bandgap (eV)	-	1.1	1.13	2.4	3.3	-
N_A (cm^{-3})	-	1×10^{15}	1×10^{15}	1×10^{13}	1×10^{13}	-
$N_D(cm^{-3})$	-	5×10^{13}	5×10^{13}	5×10^{17}	1×10^{18}	-
τ_n/τ_p(ns)	-	2.4/ 2.4	5.4/5.4	$5 \times 10^{-3}/5 \times 10^{-3}$	$3 \times 10^{-3}/ 3 \times 10^{-3}$	-
$\rho(kg/m^3)$	4690	6900	4560	4820	5610	7120
K(W/m.K)	138	103	2.95	6.2	23.4	10
C_p(J/kg.K)	277	100-130	410	210	494	340-400
$h(W/(m^2K))$	363×10^6	605×10^6	14.75×10^4	124×10^6	468×10^6	33×10^6

(300–1000 nm) was AM1.5 G, with normal incident angle only. This layer is followed by ITO layer extending upto a depth of 300 nm. The interface between ITO layer and CZTSSe layer is made by modelling ZnO and CdS layer for a thickness of 50 nm each. The thickness of CZTSSe layer is kept to be 2000 nm. This layer is further followed by $MO(S,Se)_2$ layer upto 170 nm in height followed by the last layer (Mo) which is 380 nm. The overall dimension of the cell is 400 nm × 400 nm × 3750 nm. The cell is assumed to be operating at the room temperature. Material properties are imported from COMSOL Multiphysics' material database and from the cited literature [2, 15, 16, 17, 18, 19, 23].

2.2. Meshing Configuration

The mesh configuration is similar to the previous we presented in Ref. [14]. As seen in Fig. 1 user-controlled mesh is specified for the geometry. The maximum element size is set to be 0.118 μm and minimum element size equal to 50.7 nm. The maximum element growth rate is defined to be 1.35 with curvature factor as 0.3. The resolution of narrow regions is specified to be 0.85. A swept type mesh is defined for all the domains with face-meshing method set to quadrilateral. The tessellation method is set as 'automatic'. The distribution type of the mesh elements in ZnO layer, is defined to be fixed with number of elements as 5. For CdS layer, in addition to fixed number of elements, an element ratio of 1 is specified. These two layers are the thinnest of all the other layers in geometry and thus need to be very finely meshed. The number of elements and element ratio for CZTSSe and $Mo(S,Se)_2$ is set to 70 and 0.1 respectively. Quality metrics are chosen for ensuring the mesh consistency. A measure of quality can be described based on skewness, maximum angle, volume versus circumradius, volume versus length, growth rate and condition number. In the scope of this work, skewness quality metric is chosen. The mesh quality is shown in Fig. 2. The basis of choosing this metric over others is because this metric is considered to be highly reliable and is most popular in modelling techniques. The metric defines the mesh elements according to their angular skewness. Elements with deviations from the optimal mesh (with regard to large or small angles) are penalized.

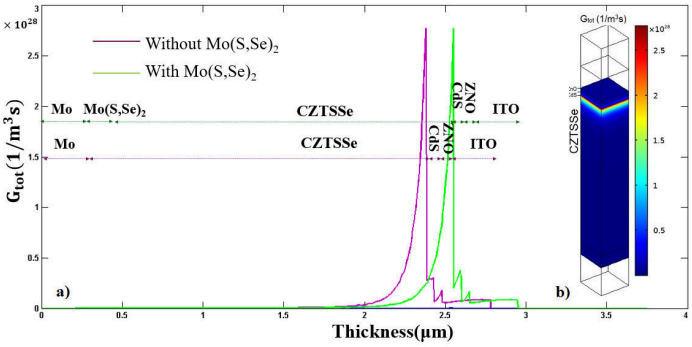

Figure 3: The total Photo-generation rate (G_{tot}) across the cell structure in a) 2D and b) 3D format out of our optical calculations in COMSOL.

Skewness close to or equal to 1 is indicative of an ideal mesh element while skewness close to 0 represents a degenerated element. Thus, based on the skewness quality metric, the defined mesh is found suitable for carrying out further analysis.

3. Results & Discussion

3.1. Optical Simulation

The optical photo-generation map of the cell has been calculated by inserting the optical constants of every layer in COMSOL environment. The refractive index and extinction coefficient of the layers were extracted from Refs. [17, 18, 19] following a Beer-Lambert optical transmission law. To enhance the photo-absorption in CZTS layer, the reflection must be minimized. However, the top layers (CdS, ZnO and ITO) have an absorption and this creates a trade-off between minimizing surface reflection and absorption in the thickness of these top layers. Fig. 3 presented the photo-generation map of the cell for a range of wavelengths between 300 nm and 1000 nm. The G_{tot} across the cell structure with and without $Mo(S,Se)_2$. We have also compared the generation rate across the cell with and without the $Mo(S,Se)_2$. The photogeneration has not changed significantly since most photons were already absorbed in CZTSSe layer and do not reach the $Mo(S,Se)_2$. Also, the latter is thin enough to have a negligible impact on G_{tot}. The same peak has been observed at the interface of CZTSSe for other CZTSSe/CdS based solar cells in Fig. 3d in Ref. [20]. Saha et al. have also reported that G_{tot} has a high peak at the CZTSe side of the interface since CZTSSe has a higher absorption compared to CdS [20]. In fact, CdS layer has a wider bandgap and absorbs high-energy photons not absorbed in CZTSSe layer and the photons with higher energy than the bandgap of CdS. Also, Abdelraouf et al. have simulated the optical photogeneration of CZTS based thin film solar cells based on coupled optical and electrical modeling (in COMSOL) and reported a same trend of 3D mapping for the G_{tot} at λ=300 nm and 800 nm [11].

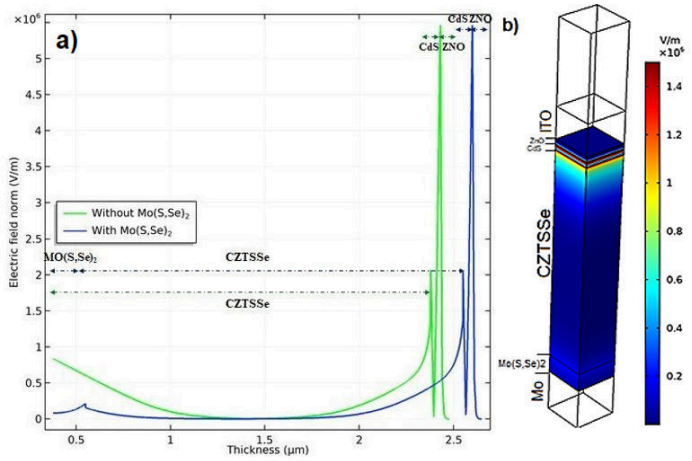

Figure 4: The Electric Field profile as extends across the cell for two structures with and without $Mo(S,Se)_2$, b) the electric field in 3D calculated from COMSOL electrical simulations coupled with optical module.

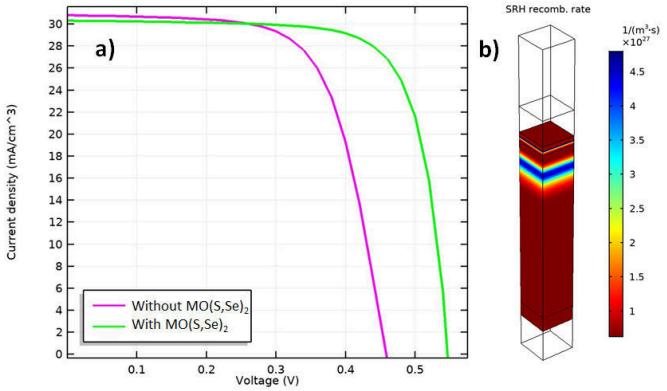

Figure 5: a) The J-V curves were calculated for both structures with and without $Mo(S,Se)_2$ layer at the bottom junction of the Mo and CZTSSe. The Mo work-function was set to 4.8 eV in electrical simulation. b) the 3D map of the SRH non-radiative recombination rate.

3.2. Electrical Simulation

The Doping profile and electrical characteristics of the modelled solar cell are presented in Table 1. At Mo/CZTSSe junction a Schottky barrier is built due to imbalance between the work functions of the Mo and CZTSSe layers. This barrier prevents the carrier transport to the Mo electrode and reduces the V_{oc}. To reduce the Schottky barrier, a thin layer of $Mo(S,Se)_2$ is introduced between the Mo and CZTSSe [21]. This thin layer will efficiently increase the V_{oc} by boosting the carrier collection at this junction. For band diagram analysis, please refer to Ref. [17]

The profile of the electric-field across the cell thickness has been also calculated in 2D as shown in Fig. 4a. By comparing the slope of electric field of the two structures in back contact regions, we observed that the $Mo(S,Se)_2$ layer decreases the electric field slope in that region. The electric field slope is directly related to bending of the band diagram at the junction through Poisson equation. From the electric field profile and the J-V curves presented later, it seems that $Mo(S,Se)_2$ balances up the band bending at Mo/CZTSSe interface and reduces the harmful effects of the Schottky contact and reduces the recombination rate therein, which in turn, boosts the V_{oc}. Moreover, the electric field shows a Lorentzian peak at the bottom interface with Mo contact where the carrier collection is improved due to the amplified electric-field to enhance the V_{oc} as also reported experimentally for such a structure in Ref. [2]. The same electric field profile has also been reported in Ref. [20] where the peaks at the interfaces is noticeable and supports an improved V_{oc}. The electric field distribution has also been shown in 3D (Fig. 4b) where the interface at the top is the most intensive and the bottom junction is less intensive not even zero electric field yet as expected from any pn junction.

Using the optical module coupled to electrical module, we have calculated the current density - voltage (J-V) characteristics of the two CZTSSe cell structures with and without $Mo(S,Se)_2$ layer (Fig. 5a). The results are in agreement with the record device metrics of the CZTSSe cell reported by IBM [2]. The IBM researchers reported V_{oc} = 0.46 V without $Mo(S,Se)_2$ layer which jumped to 0.513 V after adding this buffer layer at the junction of Mo/CZTSSe. Also, the 3D map of the SRH non-radiative recombination rate has been shown in Fig. 5b where the maximum recombination occurs within the depletion width of the CZTSSe layer near the top interface. The SRH map especially at the CZTSSe/CdS junction explains the level of obtained V_{oc}.

3.3. Thermal Simulation

Generally, in a solar cell, the majority of incident sunlight is not converted to electricity but us lost to heat generation in device. This heat can be generated via recombination and absorption mechanisms and will rise the temperature [22]. Wang et al. have also shown that non-radiative SRH recombination and thermalization are the leading energy loss in a cell [22]. Finally, we have also coupled the thermal module to the previously established optical and electrical modules in COMSOL package. The thermal analysis allows the optimization of device stability by determining which heating source is the cause of performance drop over time. We have taken several heat sources into consideration including SRH non-radiative recombination, Joule heating and the conductive heat flux magnitude (thermalization). The 3D maps of these heat generation sources have been presented in Fig. 6. Also, the 3D map of the total heat flux magnitude has been presented in order to show where the heat is emitted from the cell after all. Ahmed et. al have also shown that the interface of Mo/CZTS layers are critical for cooling the cell and keeping the temperature gradient isothermal [21]. The thermal conductivity of the $Mo(S,Se)_2$ layer is also

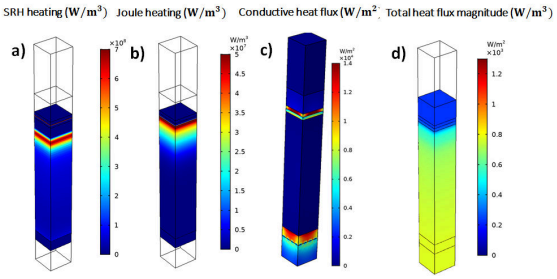

Figure 6: Thermal maps of the cell generated from different mechanisms in the cell: a) SRH recombination heat, b) Joule heating, c) heat conductive flux, and d) total heat flux magnitude.

high enough to accelerate the heat emission out of the device as stated by Peng et al. [16]. In Fig. 6c the thermal gradient at the bottom of the cell shows a high temperature within the $Mo(S,Se)_2$ layer in order of $1.2\times10^4 W/m^2$ which decreases to $0.6\times10^4 W/m^2$ in the Mo layer. In opposite, the thermal gradient at the top electrode is not intensive but is well confined in the ZnO and CdS layers and cools down rapidly when it reaches ITO and air layers on top. The total heat flux magnitude shows a more interesting trend where the thermal gradient at top electrode is non-uniform (hemisphere) shape since the heat starts to generate from the top layers by light absorption therein. The SRH heating is dominated in the bulk region of CZTSSe layer as expected due to non-radiative recombination whereas the Joule heating is 1 order of magnitude smaller here ($0.6\times10^{10} W/m^2$ vs. $0.5\times10^9 W/m^2$).

4. Conclusion

A simulation analysis has been performed on the optical, electrical, and thermal characteristics of CZTSSe thin film solar cells using COMSOL multiphysics 3D simulation package. The wave optics, semiconductor module and heat transfer in solids modules were coupled and run under a reasonably fine mesh of the cell structure. The simulation results of the optical and electrical coupled modules are in agreement with the record efficiency device parameters of the $Mo/Mo(S,Se)_2/CZTSSe/CdS/ZnO/ITO$ cell with 12.6% presented by IBM in recent years. The current-voltage characteristics of the two cells with and without $Mo(S,Se)_2$ has been compared and the open-circuit voltage of the cell with $Mo(S,Se)_2$ inserted between the Mo bottom contact and CZTSSe absorber layer shows an improvement from 0.46 V to 0.513 V in agreement with IBM record device metrics. The electric field profile displays a maximum peak at the bottom contact around the $Mo(S,Se)_2$ layer which can explain the improvement in V_{oc}. The optical generation of the two cell has not been changing much by adding the $Mo(S,Se)_2$ layer as it is a very thin buffer layer with a wide bandgap. The thermal simulation has also been performed to calculate the Shockley-Read-Hall non-radiative recombination heating, Joule heating as well as the conductive heat flux. The 3D maps of these heat generation and cooling sources helps to realize the 3D map of the total heat flux magnitude. Thermal maps show that SRH recombination heating is intensive at the depletion width on CZTSSe side, while Joule heating is intensive at the bottom electrode. A better heat conduction occurs from the MO electrode and accelerate from the $Mo(S,Se)_2$ layer. The total heat flux magnitude is more intensive at the ITO electrode and the CZTSSe/CdS interface and within the ZnO layer.

5. Acknowledgment

This research is funded by the Foundation for Science and Technology Development of Ton Duc Thang University (FOSTECT), website: http://fostect.tdtu.edu.vn, under Grant FOSTECT.2019.18.

References

[1] https://www.nrel.gov/pv/assets/pdfs/best-research-cell-efficiencies.20191106.pdf

[2] W. Wang, M. T. Winkler, O. Gunawan, T. Gokmen, T. K. Todorov, Y. Zhu, D. B. Mitzi, "Device characteristics of CZTSSe thin-film solar cells with 12.6% efficiency", *Adv. Energy Mater.*, 1-5 (2013).

[3] S.A. Khalate, R.S. Kate, R.J. Deokate, "A review on energy economics and the recent research and development in energy and the Cu_2ZnSnS_4 solar cells: A focus towards efficiency", *Solar Energy*, 169 (2018) 616-633.

[4] N. Saini, J.K. Larsen, K.V. Sopiha, (...), N. Ross, C. Platzer-Björkman, "Germanium Incorporation in Cu_2ZnSnS_4 and Formation of a Sn–Ge Gradient", *Physica Status Solidi (A) Applications and Materials Science*, 216:22 (2019) 1900492.

[5] A. Davydova, K. Rudisch, J.J.S. Scragg, "The Single Phase Region in Cu_2ZnSnS_4 Thin Films from Theory and Combinatorial Experiments", *Chemistry of Materials*, 30:14 (2018) 4624-4638

[6] A. Haddout, A. Raidou, M. Fahoume, A review on the numerical modeling of CdS/CZTS-based solar cells", *Applied Physics A*, 125:124 (2019) 1-16.

[7] A. Cherouan, R. Labbani, "Numerical simulation of CZTS solar cell with silicon back surface field", *Materials Today: Proceedings*, 5 (2018) 13795-13799.

[8] A. Cherouana, R. Labbani, "Study of CZTS and CZTSSe Solar Cells for Buffer Layers Selection", *Applied Surface Science*, 424:2 (2017) 251-255.

[9] W. Zhao, W. Zhou, X. Miao, "Numerical Simulation of CZTS Thin Film Solar Cell", *NEMS proceedings of IEEE*, Kyoto, Japan, March (2012) 502-506.

[10] O. A.M. Abdelraouf, Nageh K. Allam, " Nanostructuring for enhanced absorption and carrier collection in CZTS based solar cells: Coupled optical and electrical modeling", *Optical Materials*, 54 (2016) 84–88.

[11] O. A. M. Abdelraouf, M. I. Abdelrahaman, N. K. Allam, "Plasmonic scattering nanostructures for efficient light trapping in flat CZTS solar cells", *Proceedings of SPIE*, (2017) 10227-1022712.

[12] https://www.comsol.com/story/simulations-for-solar-42671

[13] P. Saxena, N. E. Gorji, "COMSOL Simulation of Heat Distribution in Perovskite Solar Cells: Coupled Optical-Electrical-Thermal 3D Analysis", *IEEE J. of Photovoltaics*, 9:6 (2019) 1693-1698.

[14] S. Zandi, P. Saxena, N.E. Gorji, "Numerical simulation of heat distribution in RGO-contacted perovskite solar cells using COMSOL", *Solar Energy*, 197 (2020) 105-110.

[15] S.-D. Guo, "Phonon transport in Janus monolayer MoSSe: a first-principles study", *Phys. Chem. Chem. Phys*, (2018) pccp.

[16] B. Peng, H. Zhang, H. Shao, Y. Xu, X. Zhang, H. Zhu. "Thermal conductivity of monolayer MoS_2, $MoSe_2$, and WS_2: Interplay of mass effect, interatomic bonding and anharmonicity", *RSC Adv.*, 6 (2016) 5767.

[17] D. Cozza, C. M. Ruiz, D. Duche, S. Giraldo, E. Saucedo, J. J. Simon, L. Escoubas, "Optical modeling and optimizations of $Cu_2ZnSnSe_4$ solar cells using the modified transfer matrix method", *Optics Express*, 24:18 (2016) A1201.

[18] N. Song, M. A. Green, J. Huang, Y. Hu, X. Hao, "Study of sputtered Cu_2ZnSnS_4 thin films on Si", *Applied Surface Science*, 459 (2018) 700-706.

[19] G. Reya, G. Larramonab, S. Bourdaisb, C. Chonéb, B. Delatoucheb, A. Jacobb, G. Dennlerb, S. Siebentritta, "On the origin of band-tails in kesterite", Solar Energy Materials & Solar Cells, 179 (2018) 142–151.

[20] U. Saha, Md. K. Alam, "Boosting the efficiency of single junction kesterite solar cell using Ag mixed Cu_2ZnSnS_4 active layer", *RSC Adv.*, 8 (2018) 4905-4913.

[21] M. Ahmed, X. Hao, J. Park, E. R. Hawkes, M. A. Green, "Diode Laser Annealing of CZTS Thin Film Solar Cells", *IEEE 42th proceedings*, 2015, 15664443, LA, USA.

[22] A. Wang, Y. Xuan, "A detailed study on loss processes in solar cells ", *Energy*, 144 (2018) 490-500.

[23] D. Cozza, C. Ruiz, M. Duché, J. J. Simon, L. Escoubas, "Modeling the back contact of Cu_2ZnSnS_4 solar cells" *IEEE Journal of Photovoltaics*, 6 (2016) 1292-1297.

Simulation of CZTSSe thin-film solar cells in COMSOL: three-dimensional optical, electrical, and thermal models

Zandi, Soma

2020-06-19

Zandi S, Saxena P, Razaghi M, Gorji NE. (2020) Simulation of CZTSSe thin-film solar cells in COMSOL: three-dimensional optical, electrical, and thermal models. IEEE Journal of Photovoltaics, Volume 10, Issue 5, 2020, pp.1503-1507

https://doi.org/10.1109/JPHOTOV.2020.2999881